Polytypism in $KMnCl_3$, neutron-diffraction study of the distorted-perovskite-structure compound

E. Gurewitz, M. Melamud, and A. Horowitz
Nuclear Research Centre-Negev, POB 9001, Beer-Sheva, Israel

H. Shaked
Nuclear Research Centre-Negev, POB 9001, Beer-Sheva, Israel
and Ben-Gurion University of the Negev, POB 2053, Beer-Sheva, Israel
(Received 26 March 1981; revised manuscript received 29 June 1981)

The compound $KMnCl_3$ has the interesting feature of crystallographic polytypism. Two phases were obtained, having (i) $KCdCl_3$-type structure which was previously studied and (ii) $CaTiO_3$-type (distorted-perovskite) structure. The crystallographic and magnetic structures of the $CaTiO_3$-type $KMnCl_3$ are studied. It is found that the crystallographic distortions at room temperature lead to orthorhombic symmetry (space group $Pbnm$-D_{2h}^{16}, and have components associated with the rotational normal modes M_3 and R_{25}. This phase is paramagnetic at room temperature and undergoes a transition to the antiferromagnetically ordered state at $T_N = 102\pm3$ K. The magnetic structure below T_N is a G-type structure and the magnetic moment is $4.6 \pm 0.5\mu_B$.

I. INTRODUCTION

Many of the ABX_3 compounds, where A and B are cations and X an anion, have either the ideal cubic perovskite structure (Fig. 1), or structures which are slightly distorted from the ideal one.[1–3] The compounds having distorted structures are generally of ideal cubic structure at high temperature. As the temperature is lowered, they undergo one or several transitions to increasingly distorted structures. As these distortions from the ideal cubic structure are small, it raises the interesting question whether or not these transitions are of first or second order.[4] This question had been discussed by a large number of authors.[5–12]

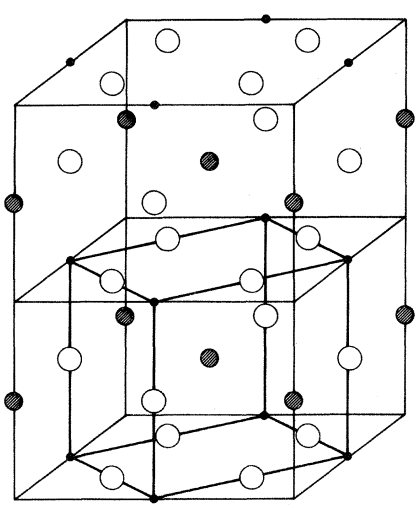

FIG. 1. The ideal cubic perovskite structure (heavy lines) and the orthorhombic (tetragonal) unit cell (light lines).

In the ideal perovskite each X ion has two B cations as neighbors forming a B-X-B angle of 180°. A slight distortion can cause only a slight change in this configuration. (In most of the distorted structures the lattice of the B cation is nearly cubic.) When X is Cl and B a magnetic transition metal, this configuration favors a negative superexchange interaction between the moments of the B ions. This leads to a G-type magnetic structure.[13] The interaction is stronger in the oxides ($X=O$) where T_N may reach several hundred degrees, whereas in the chlorides it is generally smaller than 100 °K.

Some of the $ABCl_3$ compounds have the interesting feature of crystallographic polytypism, namely the simultaneous existence of two different crystallographic structures at a given temperature range. One of the compounds possessing this property is $KMnCl_3$, which can exist at room temperature in two different orthorhombic phases.[26] The two phases have four formula units in a unit cell. One phase is isostructural with $KCdCl_3$ and has a $8.77\times3.88\times14.42 = 490.68$ Å^3 unit cell and had

been previously studied.[14] The other phase is isostructural with a distorted perovskite and has a $6.98\times7.08\times9.97 = 492.70$ Å^3 unit cell. The two phases, though structurally different, belong to the same space group, which is *Pbnm* $-D_{2h}^{16}$.

The subjects of this work are as follows

(a) Presentation of polytypism in $KMnCl_3$.

(b) Crystallographic study of the perovskite type. This type has a peseudotetragonal neutron-diffraction pattern characteristic to some other ABX_3. Therefore, this study presents analysis of such a pattern which leads to the orthorhombic *Pbnm* structure.

(c) Study of the magnetic structure of this type.

(d) A discussion of the two kinds of structural transitions that exist in this compound: (i) the transition from type to type and (ii) the transitions of the perovskite type from ideal cubic phase to orthorhombic phase. The orthorhombic structure reported here for this compound is different from the tetragonal structure reported in other works[15,16] for this phase.

II. PREPARATION

The $KMnCl_3$ sample was prepared by mixing stoichiometric amounts of the appropriate potassium and manganese chlorides in evacuated sealed quartz ampoules. The ampoules were heated to 500 °C and held at this temperature for a few hours. Because of the highly hygroscopic nature of this compound, it was handled only under dry atmosphere. Room-temperature x-ray powder diagram showed that this compound has an orthorhombic structure with lattice constants a = 6.98 Å, b = 7.08 Å, and c = 9.97 Å. This type of $KMnCl_3$ can be obtained from the $KCdCl_3$ type by heating the latter above 230 °C and cooling back to room temperature. On the other hand, hydrating the perovskitelike structure by wetting it and then dehydrating the sample at 160 °C in vacuum causes a structure change to the $KCdCl_3$ type.

III. CRYSTALLOGRAPHIC STRUCTURE — A NEUTRON-DIFFRACTION STUDY

A neutron-diffraction pattern of a powder sample of $KMnCl_3$ obtained at room temperature is presented in Fig. 2(a). The reflections are indexed according to tetragonal unit cell with dimension $a_t=\sqrt{2}a_c$ and $c_t=2a_c$, where $a_c=4.98$ Å. In the compound $KMnCl_3$, the Cl^- has the greatest ionic radius. Hence, in a hypothetical ideal cubic perovskite structure of this compound, the a_c dimension is equal to the Cl-Mn-Cl length (Fig. 1). This length is known from the $KCdCl_3$ type — $KMnCl_3$ (Table III of Ref. 14), where it is equal to $a_c=4.983$ Å. This value is very close to the a_c value (4.98 Å) deduced from the present pattern [(Fig. 2a)]. A least-squares best fit of the calculated to observed intensities using the space group *Pbnm* yielded the intensities given in Table I and position parameters which are given in Table II. The neutron-diffraction spectrum (Fig. 2) obtained for $KMnCl_3$ is characteristic of some ABX_3 compounds, such as NH_4MnCl_3 (Ref. 17) and $TlMnCl_3$ (Ref. 18).

The rest of this section deals with the analysis that had led to the use of space group *Pbnm* in analyzing the present powder diffraction.

1. The smallest cell according to which the whole spectrum can be indexed is the tetragonal cell mentioned above. In this scheme, reflections having $h+k$ odd or l odd cannot be indexed according to the ideal cubic cell ($a_c\sim5$ Å). The transformation from the ideal cubic pseudocell to the tetragonal one (Fig. 1) is $\vec{a}_t=\vec{a}_c+\vec{b}_c$, $\vec{b}_t=-\vec{a}_c+\vec{b}_c$, $\vec{c}_t=\vec{2c}_c$ and $x_t=\frac{1}{2}(x_c+y_c)$, $y_t=\frac{1}{2}(-x_c+y_c)$, $z_t=\frac{1}{2}z_c$.

2. The tetragonal unit cell does not include centering translations, as reflections with $h+k+l=2n+1$ and reflections with $h+k=2n+1$ are observed.

3. There are only two dihedral noncentered tetragonal space groups D_{4h}^1 and D_{4h}^5 which are consistent with the system of the observed reflections (Table III).

4. The partial contributions of the A, B, and X ions in the ideal cubic structure to the structure factor are given in Table IV. For positive values of scattering lengths b_A and b_X, the maximal structure factor is obtained for *EEE* (even, even, even) and *OOO* (odd, odd, odd) when $b_B>0$ and $b_B<0$, respectively. In the $KMnCl_3$ case $b_{Cl}>b_K$, $0>b_{Mn}=-b_K$, hence $|F(OOO)|>|F(EEE)|>|F(EOO)|>|F(EEO)|$. The intensity of the reflections which are related to the ideal cubic perovskite pseudocell (upper row in Fig. 2) are consistent with this inequality. This result supports the conjecture of small deviations from ideal positions. This conjecture leads to only two alternative sets of positions in each of the D_{4h}^1 and D_{4h}^5 space groups. These alternatives are given in Table V. The structure factors of the first alternative calculated for the two space groups, as well as their

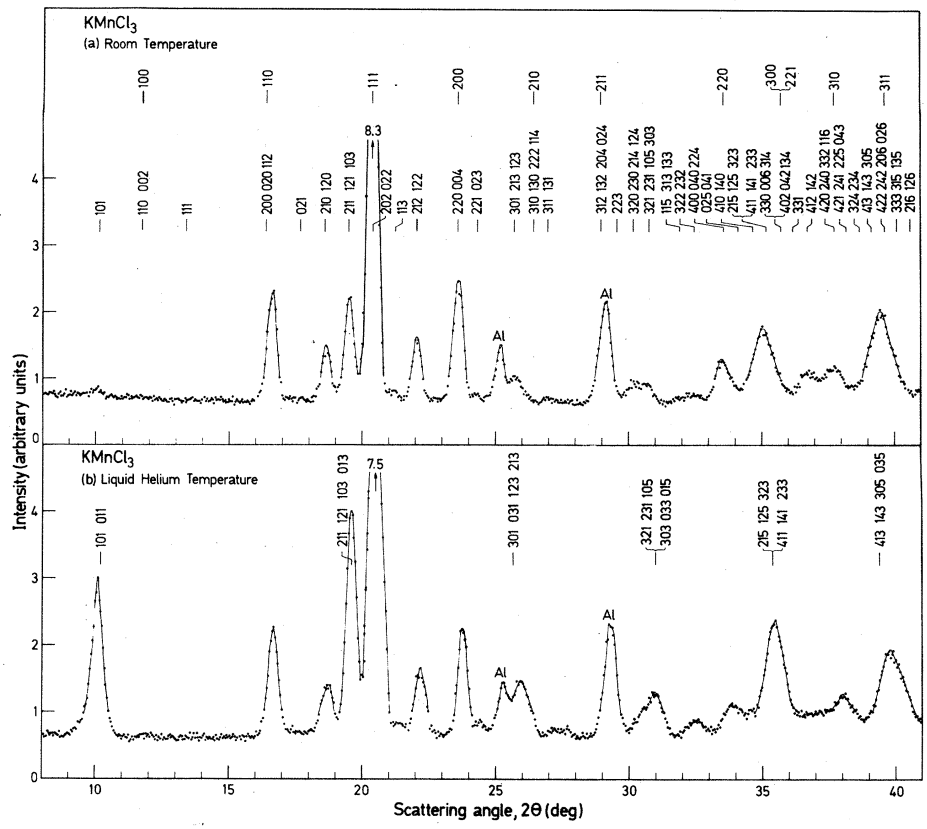

FIG. 2. Neutron- ($\lambda \sim 1.02$ Å) diffraction patterns of a powder sample of perovskite-type $KMnCl_3$ at (a) room temperature and (b) liquid-helium temperature. The indexing is according to tetragonal unit cells with $a=b=7.047$ Å, $c=a\sqrt{2}$, and $a=b=7.013$ Å, $c=a\sqrt{2}$ for (a) and (b), respectively. The upper-row indexing is according to a pseudocubic cell $a_c = 4.98$ Å. In (b) indexes of the magnetic reflections only are indicated.

derivatives, vanish at the ideal positions when $h+k=2n+1$ and $l=2n+1$. Under the conjecture of small deviations the first alternative is therefore inconsistent with the strong { 211 } observed reflection and is hence eliminated. In the second alternative the structure factor for the two space groups vanishes for odd h,k,and l. Attempts to fit the intensities calculated for this alternative in D_{4h}^1 and D_{4h}^5 to the observed spectrum were unsuccessful.

5. The above analysis shows that all the dihedral space groups D_{4h}^i $(i=1,\ldots,16)$ are inconsistent with the neutron diffraction spectrum. The next reduction (a factor of 2) in the symmetry of these space groups is to a lower primitive [see item (2) above] space group, tetragonal or dihedral orthorhombic $[D_{2h}^i$ $(i=1,\ldots,16)]$. The restrictions on space-group generators (Table III) can be carried over to tetragonal space groups of lower symmetry, many of which can therefore be excluded. From those which are subgroups of $Pm3m$, the space group for the ideal cubic perovskite, only C_{4h}^1, C_{4h}^2, D_{4h}^1, D_{4h}^2, D_{4h}^5, D_{4h}^6, C_{4v}^2, C_{4v}^1, C_{4v}^2, D_{2d}^1, D_{2d}^3, D_{2d}^5, D_{2d}^7, are left.

6. As the symmetry of the dihedral space group D_{2h}^{16}-$Pbnm$ is of the same order (multiplicity) as the symmetry of these tetragonal groups it is possible to make the following statement: There is no space group of higher symmetry than $Pbnm$ that is consistent with the observed diffraction spectrum. Furthermore, $Pbnm$ is common among many ABX_3 compounds.

This is the basis for the choice of $Pbnm$ in the analysis of the diffraction spectrum of the $KMnCl_3$ as well as $TlMnCl_3$ and NH_4MnCl_3. It shows that the choice of an orthorhombic space group can be made on the basis of the neutron diffraction although line resolution is insufficient to show it directly. As already mentioned, an orthorhombic unit cell was deduced from x-ray diffraction.[26]

There are cases where the above analysis is not

TABLE I. Comparison of calculated to observed integrated intensities of neutrons ($\lambda \sim 1.02$ Å) reflected from a powder sample of perovskite-type $KMnCl_3$ at room temperature.

$\{h\ k\ l\}$								Integrated intensites Observed	Calculated
101								72±20	51
110	002							0±20	5
111								0±20	0
200	020	112						1487±45	1521
021								20±20	43
210	120							712±35	679
211	121	103						1405±40	1420
202	022							6790±60	6726
113								74±25	69
212	122							796±45	800
220	004							1695±50	1827
221	023							73±25	77
123	213	301						557±60	536
222	310	130	114					15±20	70
311	131							56±25	60
230	320	124	214	303	321			689±55	735
133	313	115	322	232				283±50	310
400	040	224						890±10	890
025	041							135±50	107
140	410	125	215	323	233	411	141		
330	006	402	042	314	134			2237±175	2300
331	142	412	240	420	332	116	241		
421	225	043						1810±225	1464
324	234	413	143	305	422	242	206		
026	333	315	135	216	126			3152±300	2719
R (Ref.20)									0.038

strictly valid, for example, in $KMnF_3$ (Ref. 19) where the neutron-diffraction spectrum is slightly different from the spectra of these three componds. This spectrum does not exhibit strong { 210 } and { 211 } reflections and the odd h, k, and l reflections are not observed. The observed integrated intensities of its nuclear reflections[19] fit the *Pbnm* symmetry proposed in this reference with $R = 0.023$ and to the proposed[21,22] $P4/mbm$ symmetry, with $R = 0.041$. Hence, the two proposed structures fit well to the observed nuclear reflections.

IV. MAGNETIC STRUCTURE

It was found in paramagnetic resonance experiments[23,24] that $KMnCl_3$ undergoes a transition from para- to antiferromagnetic state at 100 K. Comparing the liquid-helium temperature (LHT) neutron-diffraction pattern [Fig. 2(b)] to the room-temperature (RT) pattern [Fig. 2(a)] reveals a low-temperature contribution to the reflections 101, 011; 121, 211, 103, 013; 301, 031, 213, 123; 321, 231, 105, 015, 303, 033; 215, 125, 323, 233, 411, 141. These contributions disappear upon heating

TABLE II. Parameters for $KMnCl_3$ deduced from the neutron data (observed) compared to the parameters calculated from the rotations $\zeta=0.16$ and $\eta=0.16$ rad.

Ion	Special positions	Positions parameters Observed	Calculated
Mn^{2+}	(4*b*)		
K^+	(4*c*)	$x=-0.03\pm0.02$	−0.04
		$y=0.01\pm0.01$	0.00
Cl_I^-	(4*c*)	$x=0.05\pm0.01$	0.04
		$y=0.49\pm0.01$	0.50
Cl_{II}^-	(8*d*)	$x=0.71\pm0.01$	0.71
		$y=0.29\pm0.01$	0.29
		Lattice parameters Observed	Calculated[a]
		$a=6.98$	6.99
		$b=7.08$	7.08
		$c=9.97$	9.98

[a]Normalized to $b=7.08$.

at about 100 K (see below) and are therefore due to the antiferromagnetic ordering. The indices of all these reflections are characterized by $h+k=2n+1$, $l=2n+1$. On the basis of the ideal cubic perovskite unit cell these reflections are indexed by half integers h_c, k_c, and l_c. It indicates that a_c, b_c, and c_c are antitranslations of the magnetic lattice. Such a structure, in which each moment is antiferromagnetically coupled to its six nearest neighbors, is known as a *G*-type structure.[13] Since the neutron data could not resolve the distortion in the Mn cubic lattice, it is not possible to determine with powder samples the direction of the magnetic moments.[25] The positions of the ions at LHT and the magnetic moment of the Mn^{2+} ions were calculated by a least-squares best fit of the calculated to observed intensities. The best-fitted intensities and the parameters yielding them are listed in Tables VI and VII, respectively. The best-fitted Mn^{2+} magnetic moment is $(4.6\pm0.5)\mu_B$. A study of the { 101 } reflection as a function of temperature [Fig. 3(a)] yields the transition temperature $T_N = 102\pm3$ K in agreement with the resonance experiments.[23,24] The magnetization-temperature curve deduced from the { 101 } reflection does not follow the $J=\frac{5}{2}$ Brillouin curve [Fig. 3(b)].

V. DISCUSSION

The compound $KMnCl_3$ exists in two different phases at temperatures below 230 °C. The structures of the two phases belong to the space group *Pbnm*. There is no simple transformation between

TABLE III. Possible D_{4h}^i space groups consistent with the observed reflections.

Observed reflection *h k l*	Restriction on space group generators	i=	1	2	3	4	5	6	7	8	9	10	11	12	13	14	15	16
			Possible[a] D_{4h}^i space groups															
2 1 0	$m_z\neq n$[b]		×	×			×	×				×			×	×		
1 1 3	$m_d\neq c$		×		×		×		×			×		×		×	×	×
0 4 1	$m_x(m_y)\neq c,n$		×		×		×		×		×		×		×		×	

[a]The symbol × indicates that the reflection is allowed.
[b]*n* and *c* are glide planes in the usual notation.

TABLE IV. The partial contribution of the A, B, and X ions in an ideal cubic perovskite structure to the structure factor.

Parity[a] of hkl	Contribution to structure factor by A	B	X
EEE	b_A	b_B	$3b_X$
EEO	b_A	$-b_B$	$-b_X$
EOO	b_A	b_B	$-b_X$
OOO	b_A	$-b_B$	$3b_X$

[a]E stands for even and O for odd in any permutation.

the structures of these two phases. Nevertheless, the density and volume of the unit cell are very nearly the same for the two phases. The Mn^{2+} ions in the two phases occupy octahedral sites. These octahedra are formed by the Cl^- ions and are highly distorted in the $KCdCl_3$-type phase and almost ideal in the perovskite-type phase. The octahedra are differently packed in the two phases. In the $KCdCl_3$-type phase the octahedra share a common edge, forming zigzagging chains (ZC). In the perovskite-type phase the octahedra share a common vortex (Fig. 1).

In the ZC structure the Mn^{2+} moments are located in isolated ZC and are subjected to competing interactions. These give rise to a very low 2.1-K Neel temperature, below which the compound has a spiral antiferromagnetic structure.[14] In the perovskite-type phase the magnetic moments are located in an almost cubic lattice in which the Mn-Cl-Mn angle is nearly 180°. The anitiferromagnetic interaction is strong and leads to a relatively high 102-K Neel temperature below which the compound has G-type order.[13]

The ZC phase is obtained by dehydration of $KMnCl_3 \cdot 2H_20$ at 160 °C. The perovskite type is prepared by melting stoichiometric amounts of the ingredients. A sample of a ZC phase heated almost to its melting point and cooled back to room temperature becomes a perovskite-type phase. On the other hand, a perovskite-type phase which was left for a long time in a sealed quartz ampoule changes into ZC phase. The packing of the Cl^- octahedra in the two types of structure is totally different. The transition from one type to the other requires rearrangement of the ions. This calls for a first-order transition. The mechanism which triggers these spontaneous transitions in either direction is not understood and deserves further study. These two structures and the transformations between them were also found for $TlMnCl_3$.[26]

The crystallographic structure of the perovskite-type $KMnCl_3$ is very similar to the structure of NH_4MnCl_3 and $TlMnCl_3$. The deviations of the atoms from their ideal cubic positions are small and correspond within the experimental error (Table II) to two normal modes. The two normal modes correspond to two rigid rotations of the ions in the unit cell. The rotation ζ about the z axis (Fig. 4) belongs to M_3 which corresponds to a two-dimensional representation (Fig. 5). The rotation η about the y axis results in tilting of the octahedra (Fig. 4) and belongs to one component of R_{25} which corresponds to a three-dimensional representation. The component is equal to

TABLE V. Two alternative occupations of special positions by $KMnCl_3$ ions in the two space groups D_{4h}^1 and D_{4h}^5. For a special value of the x or y parameters, a set of special positions may split into two sets of special positions of higher symmetry.

ion	D_{4h}^1 1st alternative	D_{4h}^1 2nd alternative	D_{4h}^5 1st alternative	D_{4h}^5 2nd alternative
K	$(2e)+(2f)$	$(4i)^a$	$(2c)+(2d)$	$(4f)^a$
Mn	$(2g)^a+(2h)^a$	$(a)+(b)+(c)+(d)$	$(4e)^a$	$(2a)+(2b)$
Cl_I	$(a)+(b)+(c)+(d)$	$(2g)^a+(2h)^a$	$(2a)+(2b)$	$(4e)^a$
Cl_{II}	$(8r)^{b,a}$	$(4j)^b$	$(8k)^{b,a}$	$(4g)^b$
Cl_{III}		$(4k)^b$		$(4h)^b$

[a]The z parameter of these positions is $z \sim \frac{1}{4}$.
[b]The x parameter of these positions is $x \sim \frac{1}{4}$.

TABLE VI. Comparison of calculated to observed integrated intensities of neutrons ($\lambda = 1.02$ Å) reflected from a powder sample of perovskite-type $KMnCl_3$ at liquid-helium temperature.

		$\{hkl\}$						Integrated intensities Observed	Calculated
101	011							2738±50	2724
110	002							16±20	1
111								0±20	9
200	020	112						1593±40	1594
021								60±60	1
210	120							932±35	861
211	121	103	013					3320±40	3339
202	022							6418±55	6391
113								220±60	143
212	122							1013±40	1023
220	004							1496±40	1593
221	023							352±60	301
123	213	301	031					1305±65	1281
311	131							144±45	117
223								40±40	49
230	320	124	214					321±30	344
321	231	105	015	303	033			816±45	805
133	313	115	322	232				366±40	471
400	040	224						778±45	664
025	041							160±80	155
140	410	125	215	323	233	411	141		
330	006	402	042	314	134	331		3454±100	3345
142	412	240	420	332	116	241	421		
225	043							1805±100	2020
324	234							80±80	70
413	143	305	035	422	242	206	026		
333	315	135	216	126				2975±100	2890
R (Ref.20)									0.033

TABLE VII. Parameters for $KMnCl_3$ refined with the liquid-helium temperature data.

Ion	Special positions	Positions parameters
Mn^{2+}	(4b)	
K^+	(4c)	$x = -0.02 \pm 0.01$
		$y = 0.04 \pm 0.01$
Cl_I	(4c)	$x = 0.06 \pm 0.01$
		$y = 0.50 \pm 0.01$
Cl_{II}^-	(8d)	$x = 0.70 \pm 0.01$
		$y = 0.29 \pm 0.01$
		$z = 0.04 \pm 0.01$
Mn^{2+} magnetic moment (μ_B)[a]		$\mu = 4.6 \pm 0.5$

[a]The magnetic form factor for Mn^{2+} was taken from R. E. Watson and A. J. Freeman, Acta Crystallogr. 14, 27 (1961).

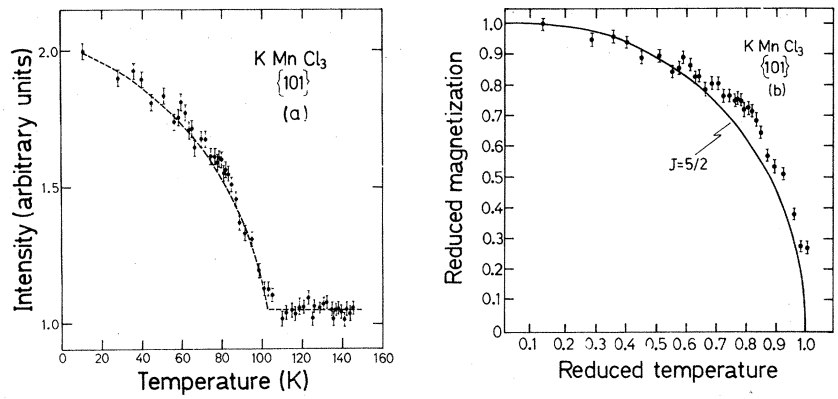

FIG. 3. (a) Temperature dependence of the peak intensity of the { 101 } magnetic reflection from powder sample of $KMnCl_3$. The broken line is a guide to the eye. (b) Reduced magnetization calculated from the { 101 } reflection vs reduced temperature. The line corresponds to Brillouin curve for $J=\frac{5}{2}$.

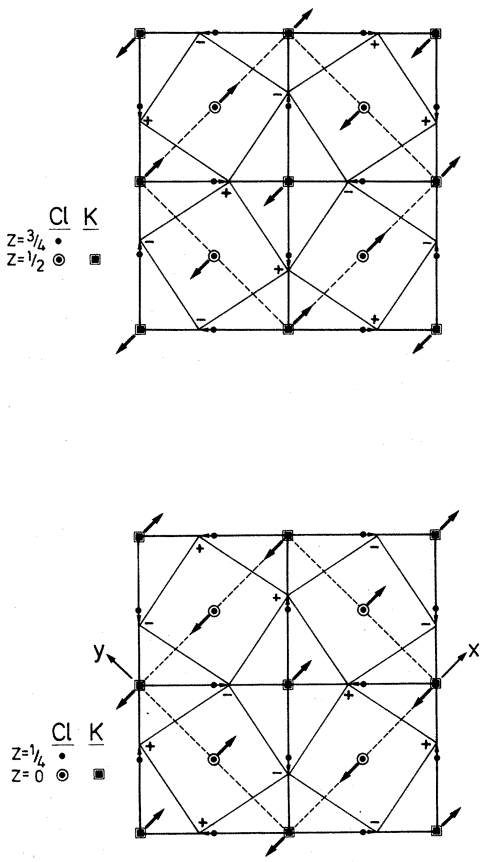

FIG. 4. Schematic drawing of the two rotations induced on the Cl^- octahedra (dotted lines) and the K^+ ions. The respective displacements of these ions from their ideal positions (black circles and squares) are indicated by arrows in the *ab* plane and $+/-$ in the *z* direction. The heavy lines are the ideal perovskite unit cell and the dashed lines are the orthorhombic unit cell.

$(\psi_x-\psi_y)/2$ (Fig. 5).

No less than nine independent parameters (seven positional and two of the lattice) are required to calculate a fit to the observed spectrum. But by applying the two rotational modes (Table VII) only two independent parameters, namely, the angles of rotations ζ and η, are needed. The seven position parameters of Table II were obtained as independent parameters best fitted to the observed data, and the lattice constants were deduced from x-ray diagrams. Comparing these nine observed parameters with their calculated values obtained by assuming $\zeta=0.16$, $\eta=0.16$ rad yields a very good agreement. This remarkable result confirms unequivocally that the crystal is driven to the distorted

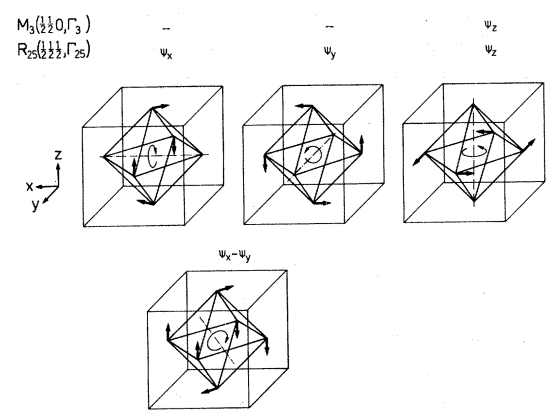

FIG. 5. Basis vectors for the two representations of $Pm\,3m$ which correspond to the observed distortions in $KMnCl_3$. A translation $(0,0,a_c)$ reverses the sign of $\psi_z(R_{25})$ but leaves $\psi_z(M_3)$ unchanged.

TABLE VIII. The distortion of the ideal cubic perovskite into the orthorhombic *Pbnm* symmetry, by application of two small rotations ζ and η around the z = [001] and y = [110] cubic axes, respectively.

Ion	Position in unit cell: Ideal cubic	Position in unit cell: Orthorhombic	Rotaion around z	Rotaion around y	Coordinates in the orthorhombic unit cell orgin at: Mn postion	Coordinates in the orthorhombic unit cell orgin at: $(\frac{1}{2},0,0)$ from Mn position	Coordinates of equivalent positions	Special position in *Pbnm*
Cl_{II}	$\pm(0,\frac{1}{2},0)$	$\pm(\frac{1}{4},\frac{1}{4},0)$	ζ	η	$\pm\frac{1}{4}(1-\zeta,1+\zeta,\bar{\eta})$	$\pm\frac{1}{4}(\bar{1}-\zeta,1+\zeta;\bar{\eta})$	$\pm(x,y,z)$	8*d*
	$\pm(\frac{1}{2},0,0)$	$\pm(\frac{1}{4},\frac{\bar{1}}{4},0)$	ζ	η	$\pm\frac{1}{4}(1+\zeta,\bar{1}+\zeta,\bar{\eta})$	$\pm\frac{1}{4}(\bar{1}+\zeta,\bar{1}+\zeta,\bar{\eta})$	$\pm(\frac{1}{2}-x,\frac{1}{2}+y,z0$	
	$\pm(0,\frac{1}{2},1)$	$\pm(\frac{1}{4},\frac{1}{4},\frac{1}{2})$	ζ	$\bar{\eta}$	$\pm\frac{1}{4}(1-\zeta,1+\zeta,2+\eta)$	$\pm\frac{1}{4}(\bar{1}-\zeta,1+\zeta,2+\eta)$	$\pm(x,y,\frac{1}{2}-z)$	
	$\pm(\frac{1}{2},0,1)$	$\pm(\frac{1}{4},\frac{\bar{1}}{4},\frac{1}{2})$	ζ	$\bar{\eta}$	$\pm\frac{1}{4}(1+\zeta,\bar{1}+\zeta,2+\eta)$	$\pm(\bar{1}+\zeta,\bar{1}+\zeta,2+\eta)$	$\pm(\frac{1}{2}-x,\frac{1}{2}+y,\frac{1}{2}-z)$	
Cl_{I}	$\pm(0,0,\frac{1}{2})$	$\pm(0,0\frac{1}{4})$	-	η	$\pm\frac{1}{4}(\eta,0,1)$	$\pm\frac{1}{4}(2+\eta,0,1)$	$\pm(x,y,\frac{1}{4})$	4*c*
	$\pm(1,0,\frac{1}{2})$	$\pm(\frac{1}{2},\frac{1}{2},\frac{1}{4})$	-	$\bar{\eta}$	$\pm\frac{1}{4}(2-\eta,2,1)$	$\pm(\eta,2,1)$	$\pm(\frac{1}{2}-x,\frac{1}{2}+y,\frac{1}{4})$	
K	$\pm(\frac{\bar{1}}{2},\frac{1}{2},\frac{1}{2})$	$\pm(0,\frac{1}{2},\frac{1}{4})$	1	$\bar{\eta}$	$\pm\frac{1}{4}(\bar{\eta},2,1)$	$\pm\frac{1}{4}(2-\eta,2,1)$	$\pm(\frac{1}{2}-x,\frac{1}{2}+y,\frac{1}{4})$	4*c*
	$\pm(\frac{1}{2},\frac{\bar{1}}{2},\frac{1}{2})$	$\pm(\frac{1}{2},0,\frac{1}{4})$	2	η	$\pm\frac{1}{4}(2+\eta,0,1)$	$\pm\frac{1}{4}(\eta,0,1)$	$\pm(x,y,\frac{1}{4})$	
Mn	(0,0,0)	(0,0,0)	-	-	(0,0,0)	$(\frac{1}{2},0,0)$	$(\frac{1}{2},0,0)$	4*b*
	(0,0,1)	$(0,0,\frac{1}{2})$	-	-	$(0,0,\frac{1}{2})$	$(\frac{1}{2},0,\frac{1}{2})$	$(\frac{1}{2},0,\frac{1}{2})$	
	(1,0,0)	$(\frac{1}{2},\frac{1}{2},0)$	-	-	$(\frac{1}{2},\frac{1}{2},0)$	$(0,\frac{1}{2},0)$	$(0,\frac{1}{2},0)$	
	(1,0,1)	$(\frac{1}{2},\frac{1}{2},\frac{1}{2})$	-	-	$(\frac{1}{2},\frac{1}{2},\frac{1}{2})$	$(0,\frac{1}{2},\frac{1}{2})$	$(0,\frac{1}{2},\frac{1}{2})$	

state by the M_3 and R_{25} modes. The angles ζ and η found in $KMnCl_3$ are both 9.17° (the equality is accidental). Similar angles were found in $KMnCl_3$ and NH_4MnCl_3. In $CaTiO_3$ these angles are[27] 9° and 11°. In the orthoferrites the angles are[28] 9°–14° and 13°–20°. The orthorhombic distortions in the orthoferrites are large compared to $KMnCl_3$ as expected, since these distortions are caused by tilting the octahedra (Fig. 5).

The high-temperature phase of the perovskite-type $KMnCl_3$ has an ideal cubic perovskite structure.[15] The transformation to the room-temperature phase takes place through three phase transitions at 458 °C,[15] 386 °C,[29] and 255 °C.[30] Several transitions are found[31] also in $TlMnCl_3$. Alexsandrov[11] proposed two sequences of phase transitions from O_h^1 to D_{2h}^{16}: (a) $O_h^1 \rightarrow D_{4h}^5 \rightarrow D_{2h}^{17} \rightarrow D_{2h}^{16}$ and (b) $O_h^1 \rightarrow D_{4h}^5 \rightarrow D_{2h}^{16}$. The $D_{4h}^4 \rightarrow D_{2h}^{17}$ transition with $k=00\frac{1}{2}$ is not of the second order. The first and second transitions in sequence (b) are induced by the condensation of M_3 and R_{25}, respectively. It would be of interest to investigate the high-temperature transitions in $KMnCl_3$ in order to find the sequence of transitions.

ACKNOWLEDGMENTS

We are indebted to Dr. S. Goshen for discussions on symmetry changes and to Mr. H. Ettedgui for his technical assistance.

APPENDIX: Explanation of Table VIII

The orthorhombically distorted unit cell contains four ABX_3 formula units. The coordinates of these 20 ions are discussed in this table. In column 2 and 3 the coordinates are given with respect to the cubic lattice (100), (010), (001) and the orthorhombic lattice (110), $(1\bar{1}0)$, (002), respectively. The A ions are subjected to ζ rotations (Fig. 5) the sum of which is zero (0). The X_I and B ions are located on some axes of rotations to which they are invariant (–). The coordinates of column 3 transform under the indicated rotations into the coordinates of column 6. A $\frac{1}{2}00$ shift of the origin yields the coordinates of column 7. The latter correspond to position parameters of column 8 in the *Pbnm* setting. The Wyckoff symbol for the corresponding special position is given in the ninth column.

[1]J. B. Goodenough and J. M. Longo, in *Landolt-Börnstein,* edited by K. H. Hellwege (Springer, Berlin, 1970), Vol. 4, p. 126.

[2]C. P. Khattak and F. F. Y. Wang, BNL Report No.

BNL-21638 (unpublished).
[3]J. Fernandez, M. J. Tello, and M. A. Arriandiaga, Mater. Res. Bull. 13, 477, 1978.
[4]L. O. Landau and E. M. Lifshitz, *Statistical Physics* (Addison-Wesley, Reading, Mass., 1969), p. 424.
[5]C. Haas, Phys. Rev. 140, 863 (1965).
[6]F. E. Goldrich and J. L. Birman, Phys. Rev. 167, 528 (1968).
[7]H. Tomas and K. A. Müller, Phys. Rev. Lett. 21, 1256 (1968).
[8]K. A. Müller, W. Berlinger, and F. Waldner, Phys. Rev. Lett. 21, 814 (1968).
[9]K. S. Aleksandrov, V. I. Zinenko, L. M. Mikhel'son, and Yu. I. Sirotin, Kristallografiya 14, 327 (1969) [Sov. Phys.—Crystallogr. 14, 256 (1968)].
[10]E. B. Vinberg, Yu. M. Gufan, V. P. Sakhnenko, and Yu. I. Sirotin, Kristallografiya 19, 21 (1974) [Sov. Phys.—Crystallogr. 19, 10 (1974)].
[11]K. S. Aleksandrov, Kristallografiya 21, 249 (1976) [Sov. Phys.—Crystallogr. 21, 133 (1976)].
[12]Yu. A. Izyumov, V. E. Naish, and V. N. Syromyatnikov, Kristallografiya 21, 256 (1976) [Sov. Phys.—Crystallogr. 21, 137 (1976)].
[13]E. F. Bertout, in *Magnetism,* edited by G. T. Rado and H. Suhl (Academic, New York, 1963), Vol. 3, pp. 149–209.
[14]E. Gurewitz, A. Horowitz, and H. Shaked, Phys. Rev. B 20, 4544 (1979).
[15]W. J. Croft, M. Kestigian, and F. D. Leipziger, Inorg. Chem. 4, 423 (1965).
[16]W. J. Croft, M. Kestigian, and F. D. Leipziger, Acta Crystallogr. 21, A-48 (1966).
[17]G. Shachar, J. Makovsky, and H. Shaked, Solid State Commun. 2, 493 (1971).
[18]M. Melamud, H. Pinto, G. Shachar, J. Makovsky, and H. Shaked, Phys. Rev. 3, 2344 (1971).
[19]V. Scatturin, L. Corliss, N. Eliott, and J. Hastings, Acta Crystallogr. 14, 19 (1961).
[20]$R=\{\sum[(I_{obs}-I_{calc})/\sigma]^2/\sum(I_{obs}/\sigma)^2\}^{1/2}$, the σ's are the estimated errors in I_{obs}.
[21]M. Hidaka, J. Phys. Jpn. 180 (1975).
[22]M. Hidaka, N. Ohama, A. Okazaki, H. Sakashita, and S. Yamakawa, Solid State Commun 16, 1121 (1975).
[23]K. Zdansdky, E. Simanek, and Z. Sroubek, Phys. Status Solidi 3, K277 (1963).
[24]R. W. Kedzie, J. R. Shane, M. Kestigian, and W. J. Croft, J. Appl. Phys. 36, 1195 (1965).
[25]G. Shirane, Acta Crystallogr. 12, 282 (1959).
[26]M. Amit and H. Horowitz (unpublished).
[27]W. Cochran and A. Zia, Phys. Status Solidi 25, 273 (1968).
[28]M. Marezio, J. P. Remeika, and P. D. Dernier, Acta Crystallogr. B 26, 2008 (1970).
[29]H. J. Seifert and F. W. Koknat, Z. Anorg, Allgem. Chem. 341, 269 (1965).
[30]A. Horowitz, M. Amit, and J. Makovsky (unpublished).
[31]I. N. Flerov, Fiz. Tverd. Tela 18, 848 (1976) [Sov. Phys.—Solid State 18, 487 (1975)].